# Enhanced antitumor and anti-metastasis efficiency via combined treatment with CXCR4 antagonist and liposomal doxorubicin

Ling Mei, Yayuan Liu, Qianyu Zhang, Huile Gao, Zhirong Zhang, Qin He *

*Key Laboratory of Drug Targeting and Drug Delivery Systems, West China School of Pharmacy, and State Key Laboratory of Biotherapy/Collaborative Innovation Center of Biotherapy, West China Hospital, Sichuan University, No. 17, Block 3, Southern Renmin Road, Chengdu 610041, PR China*

## ARTICLE INFO

## ABSTRACT

Metastasis is the main cause of cancer treatment failure and death. However, current therapies are designed to impair carcinoma metastasis mainly by impairing initial dissemination events. CXCR4 is a G-protein coupled receptor that exclusively binds its ligand CXCL12, which can stimulate cells to metastasize to distant sites. As the antagonist of chemokine receptor CXCR4, Peptide S exhibited anti-metastasis effect. In order to enhance treatment efficiency through destroying primary tumors and inhibiting their metastases, we combined PEGylated doxorubicin-loaded liposomes (DOX-Lip) with anti-metastasis Peptide S for tumor therapy for the first time. DOX-Lip exhibited similar cytotoxic activity compared to free DOX *in vitro*, and Peptide S showed no toxic effect on cell viability. However, the Peptide S sensitized CXCR4-positive B16F10 melanoma cells to DOX-Lip (5 μM) when cocultured with stromal cells (50.18 ± 0.29% of viable cells in the absence of Peptide S vs 33.70 ± 3.99% of viable cells in the presence of Peptide S). Both Peptide S and DOX-Lip inhibited the adhesion of B16F10 cells to stromal cells. We further confirmed that the inhibition of phosphorylated Akt (pAkt) by Peptide S played a key role due to the fact that activation of pAkt by DOX-Lip promoted resistance to chemotherapy. Migration and invasion assays showed that DOX-Lip enhanced anti-metastasis effect of Peptide S *in vitro* because of the cytotoxicity of doxorubicin. *In vivo* studies also showed that the combined treatment with DOX-Lip and Peptide S not only retarded primary tumor growth, but also reduced lung metastasis. Both the DOX-Lip and DOX-Lip + Peptide S exhibited even more outstanding tumor inhibition effect (with tumor growth inhibition rates of 32.1% and 37.9% respectively). In conclusion, our combined treatment with CXCR4 antagonist and liposomal doxorubicin was proved to be promising for antitumor and anti-metastasis therapy.

© 2014 Elsevier B.V. All rights reserved.

## 1. Introduction

As the primary cause of cancer-associated death, metastatic cancers are mostly incurable because of its systemic nature and the resistance of disseminated tumor cells to existing therapeutic agents [1]. 90% of mortality from cancer is attributable to metastases rather than the primary tumors from which these malignant lesions arise [2]. Conventional chemotherapy is a major therapeutic approach for the treatment of cancers which can kill most active primary or circulating tumor cells directly. For many types of cancers, cytotoxic and cytostatic drugs have achieved some success in treating primary tumors [3]. In addition, nanocarriers have been widely used to deliver chemotherapeutic drugs. Various PEGylated liposomes were studied in our lab [4–6], which could prolong circulation time and enhance the accumulation of liposomes in tumor tissues through enhanced permeability and retention (EPR) effects [7] and liposomal formulations have already been approved for human use like Doxil® and DOX-SL®. However, current cytotoxic agents and rationally designed targeted compounds often displayed only limited activity against the corresponding metastatic lesions [8]. Possible reasons for unsatisfied therapeutic effect could be due to the fact that slowly growing micrometastases can resist the effects of cytotoxic agents which principally target cells in their active growth and division cycle [9], and the neoplastic cells within metastases are intrinsically more drug-resistant than the cells in the corresponding primary tumors [10]. What's more, some researches had proved that treatment of anti-tumor drugs might increase the invasiveness of tumor cells *in vitro* [11]. Therefore, monotherapy of drug loaded nano-formulations could be ineffective to metastasized tumors, and chemotherapeutics might be an inducement of tumor metastasis.

Although many developed nano-formulations have focused on delivering apoptosis-inducing therapies to the bulk tumor, tackling cancer metastasis will require the development of novel platforms which are more specific in targeting residual cancer cells that have migrated away from the bulk tumor, rather than only debulking the main tumor mass. Cancer metastasis involves the invasion of tumor cells to blood or lymph vessels, intravasation into the vessel, extravasation from the blood vessel in another location, and invasion into the tissue to form a secondary tumor [12]. Current strategies are focused on different stages of tumor metastasis, such as anti-angiogenic agents,

* Corresponding author. Tel./fax: +86 28 85502532.
  *E-mail address:* qinhe@scu.edu.cn (Q. He).

modulating protease activity, suppressing cancer cell invasion, and so on. Among various biomolecules involved in cell invasion and metastasis, chemokine receptors play a critical role [13]. As a highly conserved transmembrane G-protein coupled receptor expressed in tumor cells, CXCR4 activated by CXCL12 can induce invasion and metastasis of many malignant tumors [14], including colorectal cancer [15], ovarian cancer [16], melanoma [17], and others. Blocking CXCL12/CXCR4 interaction may be promising therapeutics for metastases because CXCL12/CXCR4 axis triggers a variety of responses such as cell proliferation, chemotaxis and gene transcription. Small molecule inhibitors of CXCR4, like AMD3100 or blocking antibodies, are being investigated and has achieved certain anti-metastasis effect so far [18]. Recently, a new family of peptides was designed as CXCR4 antagonist, which showed anti-metastasis effect to a certain extent. Peptide S (Arg–Ala–[Cys–Arg–His–Trp–Cys]) was one of them [19]. However, these anti-metastatic therapies were designed more likely to impair initial dissemination events, and they could hardly suppress tumor growth.

Collectively, these findings further reinforced the importance of developing new approaches to inhibit the survival of primary tumor cells and the metastases. Katsuhisa et al. [20] investigated the effectiveness of the combination therapy of adriamycin (ADR) and anti-metastasis agent rh-SOD against highly metastatic clone *in vitro*. Interestingly, some studies have shown that CXCR4 inhibitor AMD3100 could disrupt tumor–stroma interactions and make them more sensitive to chemotherapeutic drugs [21,22]. These studies suggested that combined treatments of CXCR4 inhibitors and chemotherapeutic drugs might be a potential therapeutic strategy for anti-metastasis treatment. However, current researches only focused on the antitumor effects *in situ*, while the anti-metastasis efficacy and mechanism of these combination treatments were still unclear.

To explore a new strategy for enhancing antitumor and anti-metastasis efficiency, we first combined the anti-metastasis agent Peptide S with $PEG_{2000}$ modified liposomal doxorubicin (as illustrated in Fig. 1). Then we tested whether Peptide S could sensitize tumor cells to liposomal doxorubicin via CXCL12/CXCR4 axis, and the probable mechanisms were also investigated. The anti-invasion effect induced by Peptide S was then evaluated *in vitro*. Finally, the *in vivo* antitumor and anti-metastasis efficacy was studied to prove that combination therapy of liposomal doxorubicin and Peptide S could enhance anti-metastasis effect by destroying local tumor cells while Peptide S prevented cell invasion and metastasis at the same time.
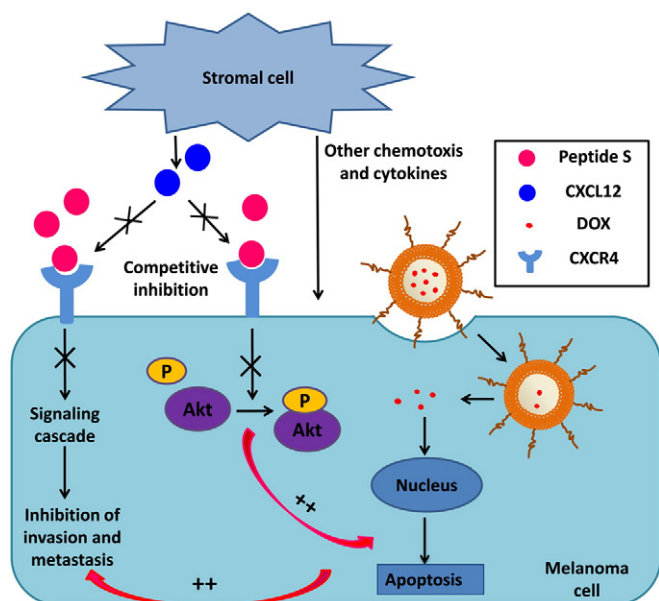


**Fig. 1.** Schematic illustration of combined treatment with Peptide S and DOX-Lip.

# 2. Materials and methods

## 2.1. Materials

Inhibitory Peptide S of CXCR4 (Arg–Ala–[Cys–Arg–His–Trp–Cys]) was synthesized according to the standard solid phase peptide synthesis by ChinaPeptides Co., Ltd. (Shanghai, China). Soybean phosphatidylcholine was purchased from Shanghai Advanced Vehicle Technology L.T.D. Co. (Shanghai,China) and Cholesterol was purchased from Kelong Chemical Company (Chengdu, China). 1, 2-distearoyl-sn-glycero-3-phosphoethanolamine-poly (ethylene glycol) 2000 ($DSPE-PEG_{2000}$) was purchased from Avanti Polar Lipids (Alabaster, AL, USA). Recombinant Murine SDF-1α/CXCL12 was obtained from PeproTech (New Jersey, USA). Cell culture inserts for 24-well plates (8.0 mm pores, Translucent PET Membrane) and BD Matrigel™ Basement Membrane Matrix were purchased from BD Biosciences (Franklin Lakes, NJ). Rabbit anti-CXCR4 polyclonal antibody and rabbit antibody against phospho-Akt (Ser473) was purchased from EnoGene (Nanjing, China). Horseradish peroxidase (HRP) -labeled goat anti-rabbit secondary antibodies were purchased from ZSGB-BIO (Beijing, China). Fluorescence probe Fluo-3 AM and Cell Counting Kit 8 were purchased from Dojindo (Beijing, China)

C57/BL6 mice (6–8 weeks old, 18–22 g) were purchased from the Experimental Animal Center of Sichuan University (Sichuan, People's Republic of China). All animal experiments for this study were approved by the Experimental Animals Administrative Committee of Sichuan University.

## 2.2. Cell lines and cell culture

Mouse metastatic melanoma cells (B16F10), human cervical carcinoma cells (Hela) and mouse fibroblast (L929) were obtained from State Key Laboratory of Biotherapy (Sichuan University) and were cultured in DMEM medium (GIBCO) supplemented with 10% FBS, 100 μg/mL streptomycin and 100 U/mL penicillin at 37 °C in a humidified incubator with 5% $CO_2$.

## 2.3. Expression of CXCR4 in B16F10 cells

The expression of CXCR4 in Hela cells and B16F10 cells was measured by Western blot studies. Approximately $5 \times 10^6$ cells were harvested, washed with cold PBS, and lysed in ice-cold lysis buffer containing protease inhibitors. The lysate was centrifuged at 14,000 rpm for 15 min at 4 °C to collect the supernatant proteins. Then appropriate total protein samples of different cells were separated by 12% SDS-PAGE and transferred to polyvinylidene difluoride membranes. After incubating with primary antibody against CXCR4, the membranes were incubated with HRP-labeled goat anti-rabbit secondary antibodies and detected by Immobilon Western HRP Substrate on a Bio-Rad ChemiDoc MP System (Bio-Rad Laboratories, USA).

## 2.4. Intracellular free $Ca^{2+}$ detection

To monitor the effect of Peptide S on intracellular calcium concentration, we used Fluo-3 AM to examine the level of intracellular free $Ca^{2+}$ of B16F10 cells. Fluo-3 AM is a fluorescent dye which could penetrate the cell membrane. After Fluo-3 AM into the cells, it can be cut into Fluo-3 by intracellular esterase and stay in the intracellular. Fluo-3 can be combined with calcium ions, and then produce strong fluorescence. After loading with the Fluo-3 dye for 30 min at 37 °C, B16F10 cells were washed with HBSS solution and exposed to CXCL12 with or without Peptide S. Detection of intracellular $Ca^{2+}$ was carried by flow cytometer (Cytomics™ FC500, Beckman Coulter, Miami, FL, USA).

## 2.5. Preparation and characterization of the DOX loaded liposomes

DOX loaded liposomes (DOX-Lip) were prepared by remote loading method, which composed of Cholesterol, Soybean phosphatidylcholine, DSPE-PEG$_{2000}$ (molar ratio = 65:33:2). The practice of detail could be seen in our laboratory previous articles [5,23].

The mean size and zeta-potential of liposomes were detected by Malvern Zetasizer Nano ZS90 (Malvern Instruments Ltd., UK). Transmission electron microscope (JEM-100CX, JEOL, Japan) was used for the morphological examination of DOX-Lip following negative staining with sodium phosphotungstate solution. Turbidity variations of DOX-Lip were monitored in 50% fetal bovine serum (FBS). The transmittance of the mixture was measured at predetermined time points at 750 nm by a microplate reader (Thermo ScientificVarioskan Flash, USA). In vitro DOX release study was performed with a dialysis method. DOX concentration was measured by a microplate reader (Thermo Scientific Varioskan Flash, USA) at Ex = 470 nm, Em = 590 nm.

## 2.6. In vitro cytotoxicity and apoptosis assay

Peptide S (0 μM, 1 μM, 10 μM, 50 μM and 100 μM) were separately added to DMEM medium of B16F10 cells in 96-well plates and incubated for 24 h. Meanwhile, free DOX and DOX-Lip with or without Peptide S (10 μM) were added to B16F10 cell layers in 96-well plates at final DOX concentrations of 0.572, 1.145, 2.29, 4.575, 9.15 and 18.3 μM per well and incubated for 24 h. After addition of 20 μL MTT solution (5 mg/mL in PBS) to each well and incubating for another 4 h, the media was removed and the crystals were dissolved by 150 μL dimethyl sulfoxide (DMSO). The absorbance was measured by Varioskan Flash Multimode Reader (Thermo, USA) at 490 nm. Cell viability (%) was calculated as A$_{test}$/A$_{control}$ × 100%. The concentration of liposomal DOX leading to 50% cell death was calculated and indicated as IC$_{50}$.

The analysis of apoptosis was performed by Annexin V-FITC/PI double staining according to the manufacturer's protocol. Briefly, B16F10 cells were seeded in 6-well plates at a density of $1 \times 10^5$/well. After incubating with free DOX and DOX-Lip (3 μM) with or without Peptide S (10 μM) for 12 h, cells were harvested, washed with cold PBS, and suspended in 500 μL binding buffer and stained by 5 μL Annexin V-FITC and 5 μL PI. The cells were incubated in the dark for 15 min and measured by flow cytometer (Cytomics$^{TM}$ FC500, Beckman Coulter, Miami, FL, USA).

## 2.7. Drug sensitivity in the coculture model

B16F10 cells were plated in 96-well plates alone, with mouse fibroblast L929 cells or chemokine CXCL12. After treating with DOX-Lip (5, 10 and 20 μM) in the presence or absence of Peptide S (10 μM) for 24 h, cell viability was detected by MTT as previously described.

## 2.8. Adhesion assay

Adhesion of B16F10 cells to the stromal cells was evaluated. Briefly, B16F10 cells were plated in the 96-well plate where L929 cells were preincubated for 12 h at 37 °C. After adding Peptide S, DOX-Lip and DOX-Lip + Peptide S for 2 h, nonadherent cells were washed gently away from the wells with PBS, and the number of adherent cells was measured by water-soluble tetrazolium salt method using Cell Counting Kit 8.

## 2.9. Akt pathway activation detected by Western blot analysis

B16F10 cells cocultured with stromal cells L929 were treated with DOX-Lip (0, 1, and 2 μM) in the presence or absence of Peptide S (10 μM) for 12 h. Subsequently, cells were homogenized with cell lysis buffer containing protease inhibitors. Western blot analyses were performed as previously described. Protein mixtures extracted from cells were separated by 10% SDS-PAGE and transferred to polyvinylidene difluoride membranes. The blots were incubated with the primary antibody against phospho-Akt and HRP-labeled goat anti-rabbit secondary antibodies subsequently, and detected by Immobilon Western HRP Substrate on a Bio-Rad ChemiDoc MP System (Bio-Rad Laboratories, USA).

## 2.10. Scratch/wound healing assay

The wound healing assay was performed similarly to those described by Shen et al. [24]. Briefly, B16F10 cells were cultured to confluence or near confluence (>90%) in 6-well plates. After scratching a straight line through the cell layer with a sterile 200-μL pipette tip, cells were incubated with DOX-Lip, Peptide S and DOX-Lip + Peptide S in DMEM medium containing 1% BSA in the presence of CXCL12 for 24 h. The images of wound closure were captured at 0 h and 24 h.

## 2.11. In vitro invasion assay

For transwell invasion assay, $1 \times 10^5$ cells were plated in the top chamber with 80 μL Matrigel-coated membranes (24-well insert, pore size: 8 μm) in DMEM medium containing 1% BSA. 100 ng/mL CXCL12 was added to the lower chamber. After incubating with DOX-Lip, Peptide S and DOX-Lip + Peptide S for 12 h, cells that did not invade through the pores were removed by a cotton swab, and the invasive cells attached to the lower surface of the membrane were fixed with 4% paraformaldehyde for 20 min and stained with crystal violet for 20 min. For quantification, cells were counted under a microscope in three randomly selected fields.

## 2.12. In vivo antitumor and anti-metastasis effect

The tumor-bearing and lung metastases models were established by subcutaneous and intravenously inoculation of $1 \times 10^6$ B16F10 cells simultaneously. For the therapeutic study, mice were randomly divided into 4 groups (n = 5): saline group (Saline), Peptide S group (Peptide S), DOX-Lip group (DOX-Lip) and the combination of Peptide S and DOX-Lip group (DOX-Lip + Peptide S). Intraperitoneal (IP) treatment started with Peptide S (2 mg/kg) every other day for 10 days. Meanwhile, all the doxorubicin preparations were injected through the tail veins at a dose of 2 mg/kg on the 7th, 11th, 15th and 19th day. On the 22nd day of tumor inoculation, mice were euthanized. Tumors and lungs were collected and photographed, followed by hematoxylin and eosin (HE) staining.

## 2.13. Statistical analysis

All the data were presented as mean ± standard deviation. Statistical comparisons were performed by one-way ANOVA for multiple groups, and $p$ value <0.05 and <0.01 were considered indications of statistical difference and statistically significant difference respectively.

# 3. Results

## 3.1. Expression of the chemokine receptor CXCR4

The expression of CXCR4 in both B16F10 cells and Hela cells (a kind of reported CXCR4-expressed cell line) was examined. Western blot analysis demonstrated definite expression of CXCR4 protein in B16F10 cells and Hela cells. The expression levels of CXCR4 were similar between the two cell lines (Fig. 2A).

## 3.2. Calcium flux

The binding of CXCL12 to CXCR4 resulting in mobilization of $Ca^{2+}$ from intracellular stores [25], which can be used to evaluate whether
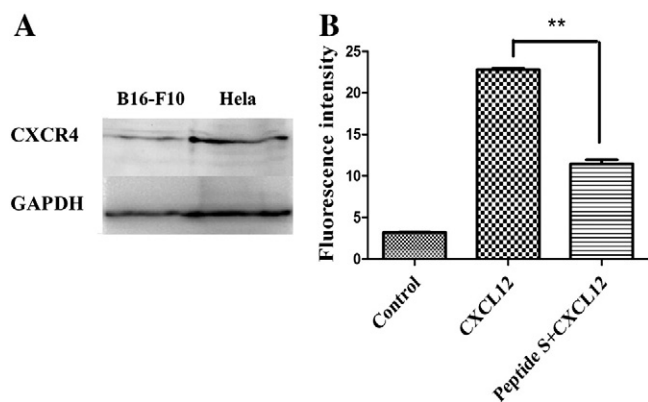
**Fig. 2.** (A) Expression of CXCR4 in Hela cells and B16F10 cells. (B) Effect of CXCL12 or Peptide S on intracellular free $Ca^{2+}$ in B16F10 cells. After being treated with CXCL12 or Peptide S +CXCL12, cells stained with Fluo-3 AM for 30 min were detected by flow cytometer analysis. Results are expressed as fluorescent intensity. ** represents the statistical significant difference ($p < 0.01$).

the inhibitory Peptide S can block the signaling pathway. In control group, the level of intracellular free $Ca^{2+}$ was the lowest (Fig. 2B). Adding CXCL12 resulted in the mobilization of $Ca^{2+}$, and the level of intracellular $Ca^{2+}$ increased. In contrast, Peptide S significantly inhibited CXCL12-induced increasing of intracellular calcium.

### 3.3. Characteristics of DOX loaded liposome

In this study, the average size of DOX-Lip was $103.4 \pm 5.5$ nm (PDI = 0.209), and the zeta potential was negatively charged ($-8.65 \pm 0.85$). Doxorubicin was successfully encapsulated in liposome with an encapsulation efficiency of $91.15 \pm 0.79\%$. TEM image, transmittance and DOX release could be seen in supporting information (Fig. S1).

### 3.4. In vitro cytotoxicity and apoptosis assay

To examine the cytotoxicity of Peptide S and DOX-Lip + Peptide S on B16F10 cells, MTT assay was performed. Fig. 3B and C showed that
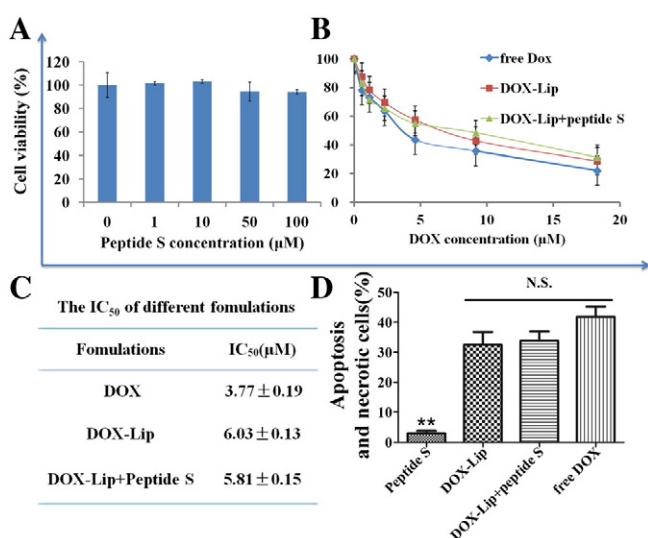
free DOX exhibited stronger inhibition effect compared to other two groups as the $IC_{50}$ value is 3.77 μM, which may be due to the reason that free drugs could be quickly transported into cells by passive diffusion with high concentration gradient [26]. The inhibition rate of DOX-Lip and DOX-Lip + Peptide S were both lower than free DOX, but there is no significant difference between the two groups (6.03 μM and 5.81 μM for DOX-Lip and DOX-Lip + Peptide S respectively) because Peptide S showed no inhibitory effect on cell viability even at concentration up to 100 μM (Fig. 3A) like other small molecular antagonists (AMD3100 [27] or TN14003[28]). The extent of apoptosis was analyzed by Annexin V-FITC/PI staining and flow cytometry in this study. As presented in Fig. 3D, the results were almost consistent with MTT assay. Peptide S could hardly induce apoptosis in B16F10 cells and didn't induce an additional effect on DOX-Lip induced apoptosis so that free DOX, DOX-Lip and DOX-Lip + Peptide S exhibited apoptosis and necrosis profiles with no noticeable difference.

### 3.5. Enhanced sensitivity of B16F10 cells to chemotherapy induced by stromal cells

To test our hypothesis that Peptide S will disrupt the interaction between stromal cells and B16F10 cells and increase their sensitivity to chemotherapeutic drugs such as doxorubicin, we examined the ability of Peptide S to overcome stromal-mediated chemoresistance of B16F10 cells. Compared to the Control group, the cell viability of B16F10 cells increased in different degrees when cocultured with L929 cells or CXCL12 at various concentrations of DOX-Lip (Fig. 4). Stromal cells are thought to be a major source of CXCL12 [22], which indicated that the protective effect of stromal cells to B16F10 cells was related to CXCL12. Furthermore, Mechanisms of stroma-mediated protection were complex and involved a variety of stroma-produced cytokines, chemokines, and adhesion molecules so that B16F10 cells exhibited higher cell viability when cultured with L929 stromal cells compared to incubation with CXCL12. Nevertheless, treatment with Peptide S decreased B16F10 cell viability compared to the Without Peptide S group whether cocultured with L929 cells or CXCL12, which due to the fact that Peptide S could competitively inhibit the binding of CXCL12 and CXCR4, and restore sensitivity of B16F10 to doxorubicin.

### 3.6. Cell adhesion assay

To test whether Peptide S enhanced the sensitivity of B16F10 cells to DOX-Lip through disrupting adhesion of B16F10 cells to the stromal cells, the effects of Peptide S, DOX-Lip, and their combination on adhesion of B16F10 cells to the L929 cells were evaluated. Fig. 5 showed that Peptide S reduced adhesion of B16F10 cells to the layer of L929 cells. Similarly, DOX-Lip also induced inhibition of B16F10 cells adhesion. However, DOX-Lip + Peptide S didn't exhibit significantly stronger inhibitory effect on adhesion compared to Peptide S or DOX-Lip alone, indicating disruption of adhesion is not the only mechanism by which Peptide S enhanced the effect of DOX-Lip.
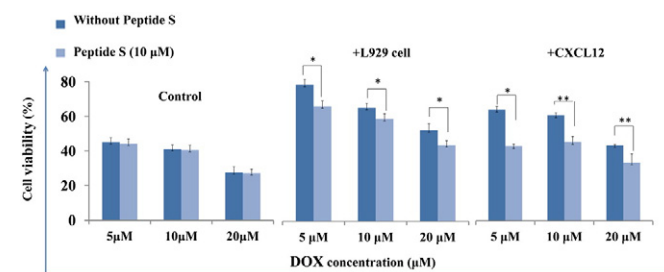


**Fig. 3.** The cytotoxicity study on B16F10 cells. (A) B16F10 cells were incubated with Peptide S at various concentrations for 24 h. Cytotoxicity was measured with MTT assay. (B) Cell viability of free DOX, DOX-Lip and DOX-Lip + Peptide S on B16F10 cells. (C) $IC_{50}$ value of different formulations. (D) The apoptosis assay on B16F10 cells after treatment with different formulations (n = 3, mean ± SD). ** represents the statistical significant difference versus other groups ($p < 0.01$).



**Fig. 4.** Viability of B16F10 cells alone (as control), with L929 stromal cells or CXCL12 and treated for 24 h with DOX-Lip in the presence of Peptide S or without Peptide S (n = 3, mean ± SD). * and ** represent $p < 0.05$ and $p < 0.01$, respectively.
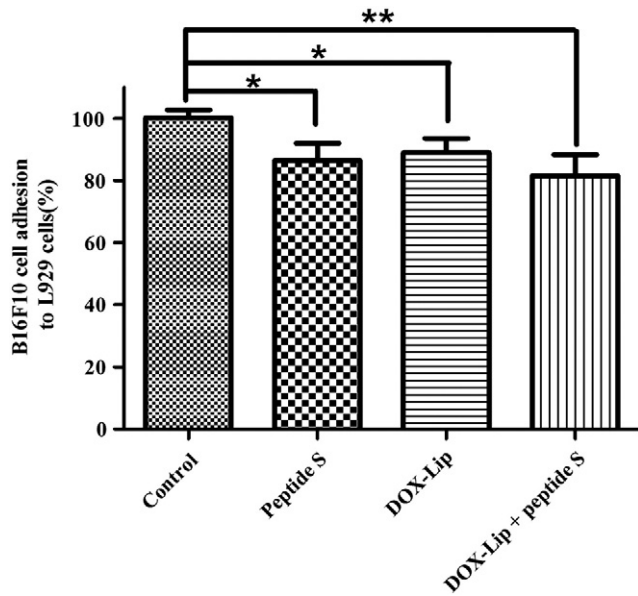
Fig. 5. The effects of Peptide S, DOX-Lip, and their combination on adhesion of B16F10 cells to L929 cells (n = 3, mean ± SD). * and ** represent $p < 0.05$ and $p < 0.01$, respectively.

### 3.7. Akt pathway activation detected by Western blot analysis

Activation of Akt kinase by phosphorylation at serine-473 prevents apoptosis in several cell systems. So we further explored this signaling mechanism. Fig. 6 showed that DOX-Lip induced a dose-dependent phosphorylation of Akt in B16F10 cells when cultured with L929 cells in the absence of Peptide S. However, DOX-Lip-mediated phosphorylation of Akt was effectively abrogated when cells were treated with Peptide S. Therefore, the antagonist Peptide S might enhance the sensitivity of B16F10 cells to DOX-Lip by inhibiting the activation of the Akt.

### 3.8. Wound healing assay

To evaluate cell motility, a wound-healing assay was performed. As showed in Fig. 7, the control group exhibited strong ability of migration and the former scratch could hardly be seen. However, treatment with Peptide S could inhibit cell migration to a certain extent while DOX-Lip showed very slight inhibitory effects. Combination treatment with Peptide S and DOX-Lip could significantly broaden the distance between the wound edges, which might be due to the DOX-Lip induced cytotoxicity effect and the decreased motility of cells by blocking CXCR4 signaling with Peptide S.

### 3.9. In vitro invasion

Tumor metastasis consists of a series of discrete biological processes that tumor cells must invade the tissue surrounding the primary tumor [8]. In vitro invasion assay was used to simulate the process. As can be seen in Fig. 8, invasion activity induced by CXCL12 (100 ng/mL) of B16F10 cells was inhibited about 34 ± 4.24% by Peptide S, but



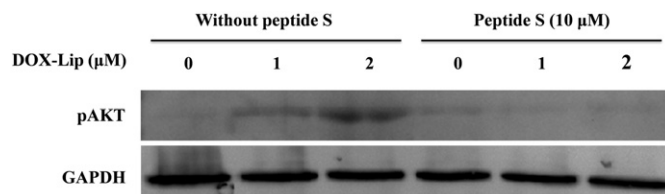Fig. 6. The effect of DOX-Lip (0, 1, and 2 μM), Peptide S (10 μM), or their combination on phosphorylation of Akt in B16F10 cells cocultured with L929 cells.
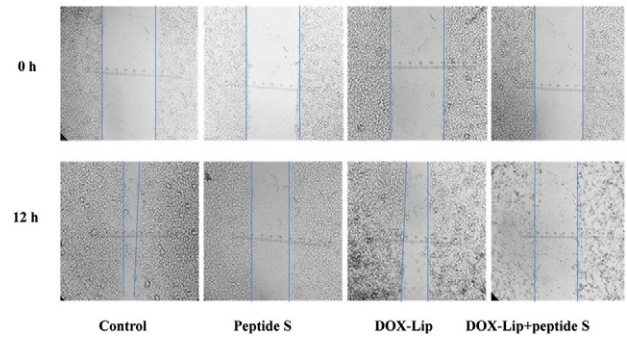


Fig. 7. Images showing the typical extent of healing of untreated B16F10 cells or treated with Peptide S, DOX-Lip and DOX-Lip + Peptide S.

treatment with DOX-Lip alone had little effect on the invasion ability. Most of all, DOX-Lip + Peptide S earned the highest activity of inhibiting B16F10 cells invasion (with an inhibition ratio of 46 ±
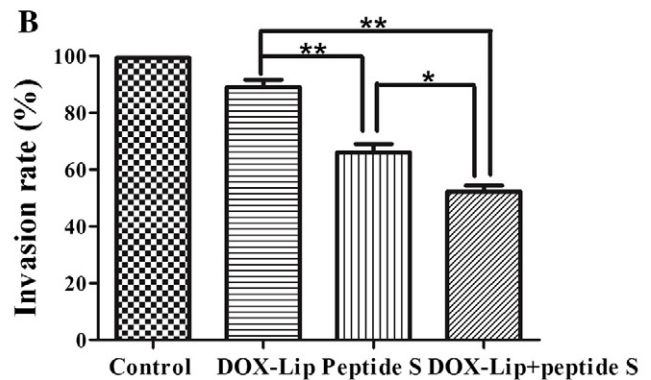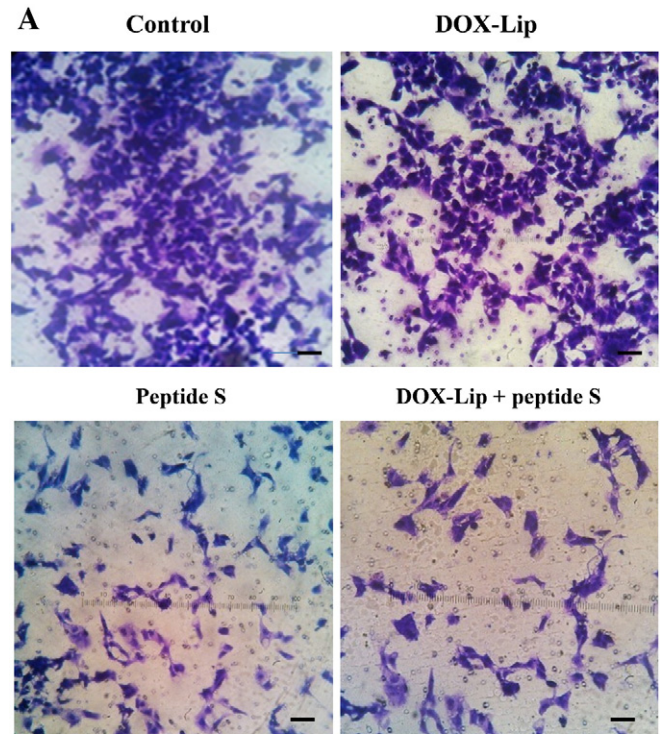


Fig. 8. (A) The representative photographs of B16F10 cells invasion after treatment with DOX-Lip, Peptide S and DOX-Lip + Peptide S. (B) Data were given as mean ± SD (n = 3). The scale bar represents 50 nm, * and ** represent $p < 0.05$ and $p < 0.01$, respectively.

1.41%), which were basically consistent with the results of the wound healing assay.

### 3.10. In vivo antitumor and anti-metastasis efficacy

The antitumor effects were evaluated on B16F10 melanoma xenografts models on C57/BL6 mice. The average tumor volumes and body weights were monitored during the experiment to monitor the antitumor efficacy and the toxicity. Mice treated with Peptide S alone showed a similar pattern and rate of tumor growth compared to saline group while DOX-Lip exhibited delayed tumor growth. Meanwhile, the combination of Peptide S and DOX-Lip also displayed a significant decrease in tumor burden (Fig. 9A, C and D). The changes in body weights of animals were also recorded as an indication of safety. The body weights of all the groups showed a slight increase during the treatment, and had no meaningful difference with each other (Fig. 9B).

After 21 days of tumor inoculation, excised lungs were almost occupied by metastasized colonies in mice treated with saline, which meant that B16F10 melanoma cells had very strong pulmonary metastasis potential. Mice treatment with DOX-Lip couldn't inhibit lung metastasis,



**Fig. 9.** Antitumor effects (A) and body weight changes (B) (n = 5, mean ± SD), * and ** represent $p < 0.05$ and $p < 0.01$, respectively. (C) and (D) represent the photographs and weights of dissected tumors at the end of treatment, * represents statistical significant difference versus saline group ($p < 0.05$), # represents statistical significant difference versus DOX-Lip + Peptide S group ($p < 0.05$). (E) and (F) represent the photographs of lungs and H&E staining sections from each group. Scale bars represent 100 µM in F.

and it was consistent with the results of *in vitro* assays, which indicated that the suppression of tumor metastasis induced by DOX-Lip was quite poor. The lung metastasis tumor was significantly reduced on the surface when treated with Peptide S and DOX-Lip + Peptide S (Fig. 9E). The hematoxylin and eosin (HE) staining images (Fig. 9F) showed clearer results. Saline group and DOX-Lip group were occupied with metastasis nodules while the lung metastasis tumor was significantly reduced by Peptide S. Furthermore, the best anti-metastasis efficacy occurred in DOX-Lip + Peptide S group. Both the area and the degree of the lung tumor burden were decreased compared with Peptide S group which was mainly because DOX-Lip affected the viability of B16F10 cells.

## 4. Discussion

The ability of chemokine receptors to facilitate metastasis in experimental settings suggests that chemokine receptor antagonists may be helpful in reducing human cancer metastasis or tumor progression [29]. Treatment of animals with various CXCR4 antagonists has resulted in considerable reduction of tumor spread in animal models of breast cancer [30], ovarian [16], and melanoma [31] metastasis. If anti-metastatic drugs do not additionally impact the behavior of already established metastases, their ultimate clinical utility will be limited. Based on this, combination therapies were reported, including combination of theanine with doxorubicin [32], oral gelatinase inhibitor with cytotoxic agent [33], and so on, which mainly aimed at inhibiting tumor growth or tumor metastasis. Here, we focused on investigating both the antitumor and anti-metastasis efficacy of combined treatment with anti-metastatic therapeutics and cytotoxic agent.

Liposomal formulations of anticancer drugs have already been approved for human use and liposomal doxorubicin showed some advantages over free doxorubicin for greater efficacy and lower cardiotoxicity [34]. The DOX-Lip used in our study had an average size around 103.4 nm and negative electricity, which are beneficial for reducing clearance and increasing circulation half-life. Meanwhile, the sustained release manner and stability in 50% FBS also laid the foundation for further *in vivo* experiments (Fig. 3B and C). Although DOX-Lip exhibited lower inhibition effect on the proliferation of B16F10 cells than free DOX (Fig. 4B), PEGylation of liposomes can avoid carriers of binding with plasma proteins and being removed by RES, thus prolonging the circulation time of carriers and making liposomes accumulate in tumor tissue via the enhanced permeability and retention (EPR) effect. That's why we chose liposomal DOX instead of free DOX.

Recent studies have reported that CXCR4 was highly expressed in malignant tumors but not normal tissue while its ligand, CXCL12, was expressed in some organs where metastases is often found (lung, liver and lymph node). Muller et al. [30] first presented data demonstrating that CXCR4 was involved in the metastasis of breast cancer cells to distant organs. The ability of chemokine receptors to facilitate metastasis in experimental settings suggests that chemokine receptor antagonists may be useful in reducing human cancer metastasis [29]. CXCL12-induced migration and invasion of cancer cells were totally blocked by inhibitors of CXCR4, such as AMD3100 [35] and TN14003 [28]. B16F10 cells (a kind of highly metastatic malignant melanoma) were selected for this study after the examination of the expression level of chemokine receptor CXCR4 by Western blot assay. As the antagonist of CXCR4, Peptide S developed by Luigi Portella et al. has shown anti-metastasis efficiency *in vitro* and *in vivo* lately. In our study, Peptide S significantly inhibited CXCL12-induced calcium efflux (Fig. 3), which demonstrated that Peptide S could block the signaling pathway. Like other inhibitor of CXCR4, Peptide S didn't induce an additional effect on DOX-Lip induced apoptosis or cell death in B16F10 cells because Peptide S showed no cytotoxicity. That's why DOX-Lip and DOX-Lip + Peptide S exhibited similar $IC_{50}$ value.

The chemo-protective role of stromal cells has been well known as one of the crucial factors affecting the response of various types of cancer cells to conventional treatment [36]. Soluble factors released by
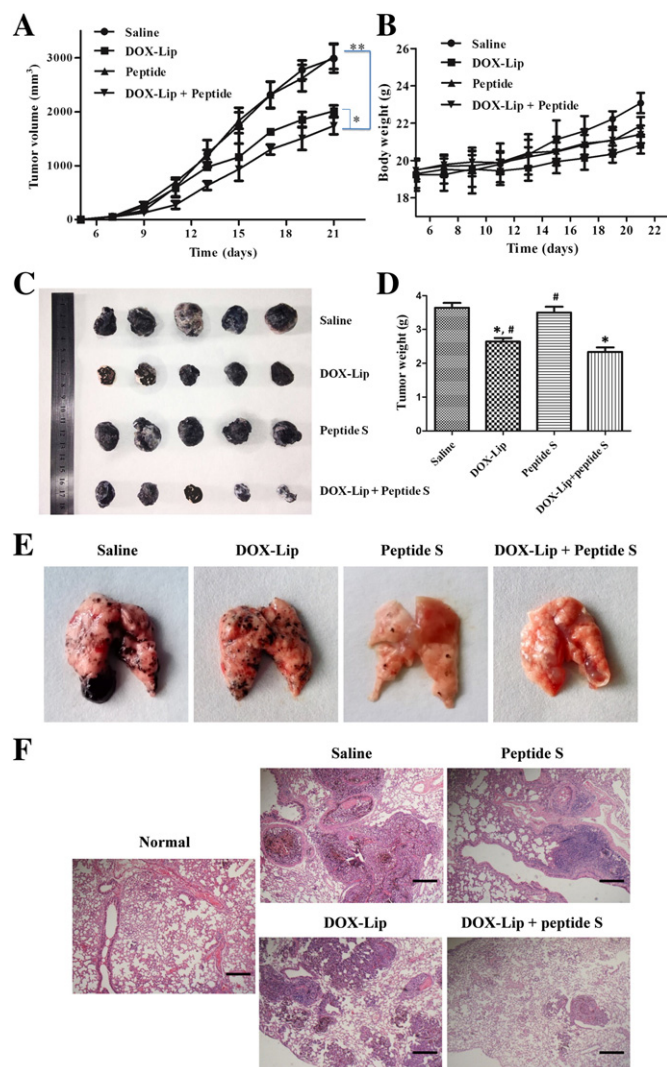
stromal cells, such as CXCL12, attracted CXCR4-expressing cancer cells to the stromal microenvironment [37]. Here, our findings indicated that Peptide S interfered with stromal/B16F10 cells interactions and sensitized them to cytotoxic therapy (Fig. 5). Moreover, we have demonstrated that the interaction between B16F10 cells and stroma was CXCL12/CXCR4 dependent and it was directly influenced by soluble CXCL12 released by stromal cells.

Cell adhesion induced chemotherapy resistance exists in many malignant cells [38,39]. Maybe Peptide S enhanced the sensitivity of B16F10 cells to DOX-Lip by disrupting adhesion of B16F10 cells to stromal cells. Thus we examined the effect of these two agents on adhesion and the results showed that Peptide S could actually reduce adhesion rate (Fig. 6). Moreover, several adhesion molecules including VCAM-1, VLA-4, and CD44 have been shown to contribute to microenvironment-mediated resistance [40,41]. For example, Zeng et al. observed sensitization of primary AML (Acute Myelocytic Leukemia) to chemotherapy via blockade of VLA-4 [42]. These findings indicated that disrupting adhesion of tumor cells to stromal cells may sensitize tumor cells to chemotherapy.

Activation of the PI3K–Akt pathway is important for cancer cells to escape cell death [43,44]. Involvement of activated PI3K–Akt signaling cascades promoting resistance against several chemotherapeutic drugs has been shown in various cell culture model systems [45–47]. In this regard, activation of the PI3K–AKT pathway is an important requirement of cancer cells to escape cell death upon exposure to toxic stimuli. What's more, PI3K can be activated by the binding of CXCL12 to CXCR4. PI3K activation can result in the phosphorylation of the serine–threonine kinase AKT [25]. We, therefore, hypothesized that Peptide S restored sensitivity of cells to DOX-Lip induced apoptosis or cell death through the inhibition of the PI3K–Akt signaling pathway. Subsequent experiments confirmed that DOX-Lip induced a dose-dependent increase of pAkt in B16F10 cells when cocultured with L929 cells, but Peptide S abolished the increase in phosphorylation of Akt, indicating a potential mechanism by which Peptide S enhanced the sensitivity of B16F10 cells to chemotherapy via inhibiting PI3K–Akt pathway (Fig. 7). There are other possible mechanisms related to chemosensitization. CXCL12 can promote cell survival through the MAP-kinase cascades, and both p38 and Erk1/2 have been implicated in tumor cell survival, too [48]. But these signaling pathways make little contribution to cell survival or proliferation.

As for anti-metastasis efficiency, *in vitro* invasion activity of B16F10 cells determined by transwell assay was similar to wound healing assay. Because of the distinct mechanisms of these two agents for cancer therapy, it's no surprise that Peptide S significantly inhibited migration or invasion activity of B16F10 cells while cytotoxic formulation DOX-Lip didn't. DOX-Lip + Peptide S exhibited stronger ability of inhibiting B16F10 cells migration or invasion compared to treatment with Peptide S alone. We next investigated whether this therapy was effective against lung metastases of melanoma *in vivo*. On the tumor-bearing and experimental melanoma lung metastases model, DOX-Lip led to significantly better antitumor effect compared to saline group or Peptide S group. In contrast, the lungs of Peptide S-treated mice showed less of tumor metastasis. But most important of all, the enhanced antitumor and anti-metastasis efficacy of combined treatment was obtained with no obvious accompanied toxicity. In addition, our study showed clinical potential because liposomal doxorubicin has already been approved for clinical use and phase I trial was planned with Peptide S in patients for advanced tumors [19].

## 5. Conclusions

In summary, inhibitory Peptide S of CXCR4 disrupted the interaction of B16F10 cells with stroma through CXCL12/CXCR4 axis and inhibited the DOX-Lip induced PI3K/Akt signaling, leading to enhanced sensitivity of B16F10 cells to DOX-Lip. Moreover, *in vitro* and *in vivo* enhanced anti-metastases efficiency were examined by combined treatment with

Peptide S and DOX-Lip due to the fact that DOX-Lip killed primary tumor cells while Peptide S inhibited migration and invasion. In view of this, our findings set the stage for clinical trials with combined treatment of conventional chemotherapy and CXCR4 antagonists, with the ultimate aim of improving treatment outcome in highly metastatic melanoma.

Supplementary data to this article can be found online at http://dx.doi.org/10.1016/j.jconrel.2014.10.017.

## References

[1] S. Valastyan, R.A. Weinberg, Tumor metastasis: molecular insights and evolving paradigms, Cell 147 (2) (2011) 275–292.
[2] G.P. Gupta, J. Massagué, Cancer metastasis: building a framework, Cell 127 (4) (2006) 679–695.
[3] R.B. Ewesuedo, M.J. Ratain, Oncologic Therapies, Springer, 2003. 19–66.
[4] R. Kuai, W. Yuan, Y. Qin, H. Chen, J. Tang, M. Yuan, Z. Zhang, Q. He, Efficient delivery of payload into tumor cells in a controlled manner by TAT and thiolytic cleavable PEG co-modified liposomes, Mol. Pharm. 7 (5) (2010) 1816–1826.
[5] J. Tang, H. Fu, Q. Kuang, L. Zhang, Q. Zhang, Y. Liu, R. Ran, H. Gao, Z. Zhang, Q. He, Liposomes co-modified with cholesterol anchored cleavable PEG and octaarginines for tumor targeted drug delivery, J. Drug Target. (0) (2014) 1–14.
[6] Y. Liu, R. Ran, J. Chen, Q. Kuang, J. Tang, L. Mei, Q. Zhang, H. Gao, Z. Zhang, Q. He, Paclitaxel loaded liposomes decorated with a multifunctional tandem peptide for glioma targeting, Biomaterials 35 (17) (2014) 4835–4847.
[7] T.M. Allen, C.B. Hansen, D.E.L. de Menezes, Pharmacokinetics of long-circulating liposomes, Adv. Drug Deliv. Rev. 16 (2) (1995) 267–284.
[8] P.S. Steeg, Tumor metastasis: mechanistic insights and clinical challenges, Nat. Med. 12 (8) (2006) 895–904.
[9] J.A. Aguirre-Ghiso, Models, mechanisms and clinical evidence for cancer dormancy, Nat. Rev. Cancer 7 (11) (2007) 834–846.
[10] J.P. Thiery, H. Acloque, R.Y. Huang, M.A. Nieto, Epithelial-mesenchymal transitions in development and disease, Cell 139 (5) (2009) 871–890.
[11] Y. Liang, P. Meleady, I. Cleary, S. McDonnell, L. Connolly, M. Clynes, *Selection with melphalan or paclitaxel (Taxol) yields variants with different patterns of multidrug resistance, integrin expression and < i > in vitro* invasiveness, Eur. J. Cancer 37 (8) (2001) 1041–1052.
[12] T.D. Palmer, W.J. Ashby, J.D. Lewis, A. Zijlstra, Targeting tumor cell motility to prevent metastasis, Adv. Drug Deliv. Rev. 63 (8) (2011) 568–581.
[13] F. Balkwill, Cancer and the chemokine network, Nat. Rev. Cancer 4 (7) (2004) 540–550.
[14] J.A. Burger, T.J. Kipps, CXCR4: a key receptor in the crosstalk between tumor cells and their microenvironment, Blood 107 (5) (2006) 1761–1767.
[15] I.S. Zeelenberg, L. Ruuls-Van Stalle, E. Roos, The chemokine receptor CXCR4 is required for outgrowth of colon carcinoma micrometastases, Cancer Res. 63 (13) (2003) 3833–3839.
[16] C.J. Scotton, J.L. Wilson, K. Scott, G. Stamp, G.D. Wilbanks, S. Fricker, G. Bridger, F.R. Balkwill, Multiple actions of the chemokine CXCL12 on epithelial tumor cells in human ovarian cancer, Cancer Res. 62 (20) (2002) 5930–5938.
[17] S. Scala, A. Ottaiano, P.A. Ascierto, M. Cavalli, E. Simeone, P. Giuliano, M. Napolitano, R. Franco, G. Botti, G. Castello, Expression of CXCR4 predicts poor prognosis in patients with malignant melanoma, Clin. Cancer Res. 11 (5) (2005) 1835–1841.
[18] J.A. Burger, A. Peled, CXCR4 antagonists: targeting the microenvironment in leukemia and other cancers, Leukemia 23 (1) (2009) 43–52.
[19] L. Portella, R. Vitale, S. De Luca, C.D. Alterio, C. Ieranò, M. Napolitano, A. Riccio, M.N. Polimeno, L. Monfregola, A. Barbieri, Preclinical development of a novel class of CXCR4 antagonist impairing solid tumors growth and metastases, PLoS One 8 (9) (2013) e74548.
[20] K. Kogawa, H. Muramatsu, M. Tanaka, Y. Nishihori, S. Hagiwara, K. Kuribayashi, K. Nakamura, K. Koike, S. Sakamaki, Y. Niitsu, Enhanced inhibition of experimental metastasis by the combination chemotherapy of Cu–Zn SOD and adriamycin, Clin. Exp. Metastasis 17 (3) (1999) 239–244.
[21] A.K. Azab, J.M. Runnels, C. Pitsillides, A. Moreau, F. Azab, X. Leleu, X. Jia, R. Wright, B. Ospina, A.L. Carlson, CXCR4 inhibitor AMD3100 disrupts the interaction of multiple myeloma cells with the bone marrow microenvironment and enhances their sensitivity to therapy, Blood 113 (18) (2009) 4341–4351.
[22] U.M. Domanska, H. Timmer-Bosscha, W.B. Nagengast, T.H.O. Munnink, R.C. Kruizinga, H.J. Ananias, N.M. Kliphuis, G. Huls, E.G. De Vries, I.J. de Jong, CXCR4 inhibition with AMD3100 sensitizes prostate cancer to docetaxel chemotherapy, Neoplasia 14 (8) (2012) 709.
[23] T. Zong, L. Mei, H. Gao, W. Cai, P. Zhu, K. Shi, J. Chen, Y. Wang, F. Gao, Q. He, Synergistic dual-ligand doxorubicin liposomes improve targeting and therapeutic efficacy of brain glioma in animals, Mol. Pharm 11 (7) (2014) 2346–2357.
[24] J. Shen, H. Sun, P. Xu, Q. Yin, Z. Zhang, S. Wang, H. Yu, Y. Li, Simultaneous inhibition of metastasis and growth of breast cancer by co-delivery of twist shRNA and

paclitaxel using pluronic P85-PEI/TPGS complex nanoparticles, Biomaterials 34 (5) (2013) 1581–1590.

[25] B.A. Teicher, S.P. Fricker, CXCL12 (SDF-1)/CXCR4 pathway in cancer, Clin. Cancer Res. 16 (11) (2010) 2927–2931.

[26] J. Yao, L. Zhang, J. Zhou, H. Liu, Q. Zhang, Efficient simultaneous tumor targeting delivery of all-trans retinoid acid and paclitaxel based on hyaluronic acid-based multifunctional nanocarrier, Mol. Pharm. 10 (3) (2013) 1080–1091.

[27] D. Uchida, T. Onoue, Y. Tomizuka, N.M. Begum, Y. Miwa, H. Yoshida, M. Sato, Involvement of an autocrine stromal cell-derived factor-1/CXCR4 system on the distant metastasis of human oral squamous cell carcinoma, Mol. Cancer Res. 5 (7) (2007) 685–694.

[28] T. Mori, R. Doi, M. Koizumi, E. Toyoda, D. Ito, K. Kami, T. Masui, K. Fujimoto, H. Tamamura, K. Hiramatsu, CXCR4 antagonist inhibits stromal cell-derived factor 1-induced migration and invasion of human pancreatic cancer, Mol. Cancer Ther. 3 (1) (2004) 29–37.

[29] T. Murakami, A.R. Cardones, S.T. Hwang, Chemokine receptors and melanoma metastasis, J. Dermatol. Sci. 36 (2) (2004) 71–78.

[30] A. Müller, B. Homey, H. Soto, N. Ge, D. Catron, M.E. Buchanan, T. McClanahan, E. Murphy, W. Yuan, S.N. Wagner, Involvement of chemokine receptors in breast cancer metastasis, Nature 410 (6824) (2001) 50–56.

[31] T. Murakami, W. Maki, A.R. Cardones, H. Fang, A.T. Kyi, F.O. Nestle, S.T. Hwang, Expression of CXC chemokine receptor-4 enhances the pulmonary metastatic potential of murine B16 melanoma cells, Cancer Res. 62 (24) (2002) 7328–7334.

[32] T. Sugiyama, Y. Sadzuka, Combination of theanine with doxorubicin inhibits hepatic metastasis of M5076 ovarian sarcoma, Clin. Cancer Res. 5 (2) (1999) 413–416.

[33] I.C. Anderson, M.A. Shipp, A.J. Docherty, B.A. Teicher, Combination therapy including a gelatinase inhibitor and cytotoxic agent reduces local invasion and metastasis of murine Lewis lung carcinoma, Cancer Res. 56 (4) (1996) 715–718.

[34] A.A. Gabizon, Liposome circulation time and tumor targeting: implications for cancer chemotherapy, Adv. Drug Deliv. Rev. 16 (2) (1995) 285–294.

[35] J. Li, Y. Zhu, S.T. Hazeldine, C. Li, D. Oupický, Dual-function CXCR4 antagonist polyplexes to deliver gene therapy and inhibit cancer cell invasion, Angew. Chem. Int. Ed. 51 (35) (2012) 8740–8743.

[36] M.B. Meads, L.A. Hazlehurst, W.S. Dalton, The bone marrow microenvironment as a tumor sanctuary and contributor to drug resistance, Clin. Cancer Res. 14 (9) (2008) 2519–2526.

[37] Y. Nefedova, T.H. Landowski, W.S. Dalton, Bone marrow stromal-derived soluble factors and direct cell contact contribute to de novo drug resistance of myeloma cells by distinct mechanisms, Leukemia 17 (6) (2003) 1175–1182.

[38] T. Hikawa, T. Mori, T. Abe, S. Hori, The ability in adhesion and invasion of drug-resistant human glioma cells, J. Exp. Clin. Cancer Res. 19 (3) (2000) 357–362.

[39] G. Kouniavsky, M. Khaikin, I. Zvibel, D. Zippel, S. Brill, Z. Halpern, M. Papa, Stromal extracellular matrix reduces chemotherapy-induced apoptosis in colon cancer cell lines, Clin. Exp. Metastasis 19 (1) (2002) 55–60.

[40] T. Matsunaga, N. Takemoto, T. Sato, R. Takimoto, I. Tanaka, A. Fujimi, T. Akiyama, H. Kuroda, Y. Kawano, M. Kobune, Interaction between leukemic-cell VLA-4 and stromal fibronectin is a decisive factor for minimal residual disease of acute myelog-enous leukemia, Nat. Med. 9 (9) (2003) 1158–1165.

[41] L. Jin, K.J. Hope, Q. Zhai, F. Smadja-Joffe, J.E. Dick, Targeting of CD44 eradicates human acute myeloid leukemic stem cells, Nat. Med. 12 (10) (2006) 1167–1174.

[42] Z. Zeng, Y.X. Shi, I.J. Samudio, R. Wang, X. Ling, O. Frolova, M. Levis, J.B. Rubin, R.R. Negrin, E.H. Estey, Targeting the leukemia microenvironment by CXCR4 inhibition overcomes resistance to kinase inhibitors and chemotherapy in AML, Blood 113 (24) (2009) 6215–6224.

[43] B.D. Manning, L.C. Cantley, AKT/PKB signaling: navigating downstream, Cell 129 (7) (2007) 1261–1274.

[44] T.L. Yuan, L.C. Cantley, PI3K pathway alterations in cancer: variations on a theme, Oncogene 27 (41) (2008) 5497–5510.

[45] M. Bezler, J.G. Hengstler, A. Ullrich, Inhibition of doxorubicin-induced HER3–PI3K–AKT signalling enhances apoptosis of ovarian cancer cells, Mol. Oncol. 6 (5) (2012) 516–529.

[46] L. Liu, X. Zhou, G. Qian, X. Shi, J. Fang, B. Jiang, AKT1 amplification regulates cisplatin resistance in human lung cancer cells through the mammalian target of rapamycin/p70S6K1 pathway, Cancer Res. 67 (13) (2007) 6325–6332.

[47] X. Li, Y. Lu, K. Liang, B. Liu, Z. Fan, Differential responses to doxorubicin-induced phosphorylation and activation of Akt in human breast cancer cells, Breast Cancer Res. 7 (5) (2005) R589–R597.

[48] S.R. Vlahakis, A. Villasis-Keever, T. Gomez, M. Vanegas, N. Vlahakis, C.V. Paya, G protein-coupled chemokine receptors induce both survival and apoptotic signaling pathways, J. Immunol. 169 (10) (2002) 5546–5554.